Phenotypic evolution of circulating plasma cells from early precursor stages to multiple myeloma

Martin Pietzsch,[1*] Sina Alexandra Beer,[1*] Lucca Marco Kimmich,[1] Chiara Windsor,[1] Sarah Gekeler,[1] Britta Besemer[1] and Anna Maria Paczulla Stanger[1,2]

[1]University Clinic Tübingen, Department for Internal Medicine II, University of Tübingen and [2]Flow Cytometry Core Facility, Medical Faculty Tübingen, University of Tübingen, Tübingen, Germany

**MP and SAB contributed equally as first authors.*

Correspondence: A.M. Paczulla Stanger
Anna.Stanger@med.uni-tuebingen.de

Received: October 26, 2025.
Accepted: March 11, 2026.
Early view: April 2, 2026.

https://doi.org/10.3324/haematol.2025.300105

Published under a CC BY license

Abstract

Circulating tumor plasma cells (CTPC) have emerged as valuable diagnostic and prognostic marker in multiple myeloma (MM), with their presence linked to progression from precursor stages and poorer outcomes in newly diagnosed MM (NDMM). While quantitative CTPC enumeration is increasingly validated, comprehensive phenotypic profiling across disease stages remains lacking. We applied 36-parameter spectral flow cytometry to 113 peripheral blood mononuclear cell samples of monoclonal gammopathy of undetermined significance (N=42), smouldering MM (N=22), NDMM (N=15), treated MM (N=24), and healthy controls (N=10), alongside paired bone marrow (BM) samples from six NDMM patients. CTPC were defined phenotypically as $CD45^{-}CD38^{high}CD56^{+}$ events without assessment of clonality. Phenotypic profiling of the $CD56^{+}$ CTPC-like subset across disease stages revealed alterations in canonical and lineage-atypical surface markers. Progression to NDMM was characterized by upregulation of CD38 and CD56 with concomitant loss of B- (CD19), myeloid- (CD14, CD16), and T-cell-associated (CD45RA) markers. In addition, HLA-ABC, interleukin receptor subunits (CD25, CD123), and chemokine receptors (CCR6, CCR7) were upregulated in NDMM. In treated MM, a reversed pattern was observed with lower CD25 and CD123 expression and increased levels of exhaustion markers (TIGIT, PD-1). Paired BM samples showed a different tissue-residency marker expression, characterized by higher CD69 and CCR6 and lower CD138, along with changes in cell-survival related markers, including increased CD25 and CD123. Both BCMA and CD307e were more highly expressed on BM plasma cells than CTPC. This study is among the first to provide a comprehensive phenotypic characterization of $CD56^{+}$ CTPC across the MM spectrum, including checkpoint and chemokine receptors, treated disease cases, and paired BM samples for NDMM.

Introduction

Multiple myeloma (MM) is a plasma cell dyscrasia characterized by the clonal proliferation of malignant plasma cells (PC) within the bone marrow (BM), leading to abnormal immunoglobulin production and progressive skeletal destruction. In most cases, MM evolves from precursor conditions such as monoclonal gammopathy of undetermined significance (MGUS) and smouldering MM (SMM), which can persist for years before overt malignancy develops.[1,2] Disease progression is likely driven by a dynamic crosstalk between malignant PC and the tumor microenvironment (TME), promoting sub-clonal evolution as well as invasion across various BM niches and beyond.[3] In long-standing precursor lesions, chronic immune activation likely exposes the immune system to tumor-associated neoantigens over many years, leading to immune dysfunction and T-cell exhaustion.[3,4] However, the underlying biology including the timely pattern of disease progression remains poorly understood. Current risk-stratification models, despite recent advances, still have limitations in predicting which patients with MGUS or SMM will progress to symptomatic MM,[5,6] underscoring the need for more precise biomarkers. Circulating tumor plasma cells (CTPC) have emerged as a powerful diagnostic and prognostic tool in MM. Using spectral flow cytometry (SFC), CTPC can be detected in the peripheral blood (PB) of virtually all newly diagnosed MM (NDMM) patients and, depending on assay sensitivity, reliably identified in precursor conditions.[7] Their presence is associated with progression in MGUS and SMM and is linked to poorer outcomes in NDMM, although definitive cut-offs still need to be established.[8,9] Interestingly, high CTPC counts are observed to be associated with a distinct immune profile in both PB and TME (e.g., higher levels of

cytotoxic T/NK cells and tumor-associated macrophages, increased memory/naive B-cell ratio).[10,11] Yet, while quantitative CTPC enumeration is increasingly validated, comprehensive phenotypic profiling of CTPC themselves across disease stages is lacking.

In this study, we leveraged high-parameter spectral flow cytometry in a real-world cohort of MGUS, SMM, NDMM, and treated MM patients to delineate CTPC phenotypic evolution across disease stages. Our aim was to uncover biomarkers in precursor conditions and advance our understanding of myeloma biology.

Methods

Study population and clinical data acquisition

We conducted a cross-sectional study including adult patients with MGUS, SMM, NDMM or treated MM in an outpatient care setting at the department of Internal Medicine II, University Hospital Tübingen. From February 2022 to July 2023, we obtained peripheral blood mononuclear cell (PBMC) samples from 103 patients, who met flow cytometry quality control criteria (i.e., sufficient viable cell counts for staining and measurement, circulating plasma cell [CPC] count over limit of detection) and study inclusion criteria (Figure 1). Six matched BM aspirates of NDMM patients were collected. Ten fully anonymized healthy blood-bank donors served as controls.

For MGUS, SMM and MM patients, electronic medical records were reviewed regarding disease subtype, therapy lines, remission status (defined based on the International Myeloma Working Group [IMWG] criteria), and laboratory findings. Risk stratification was performed using the Mayo Clinic MGUS Risk Stratification Model,[12] the IMWG 2/20/20 model for SMM,[6] and the updated IMS/IMWG high-risk guidelines for MM patients.[13]

Analysis of multiparameter spectral flow cytometry

PBMC were enriched by density gradient centrifugation and viably frozen.

Single-cell suspensions from PBMC of patients were stained with fluorescently labeled antibodies (see *Online Supplementary Table S1* and the *Online Supplementary Appendix* for more details). For spectral unmixing, a combination of both single stained cells and UltraComp eBeads™ Plus Compensation Beads (ThermoFisher) was applied. Dead cells were excluded using LIVE/DEAD™ Fixable Blue Dead Cell Staining dye (ThermoFisher). The panel and gating strategy were adapted from the OMIP-069 immunophenotyping protocol.[14] Samples were acquired using a Cytek AURORA spectral flow cytometer enabling simultaneous detection of all cell types and qualitative markers. Analysis was performed with Cytolution Software (from Cytolytics GmbH) using manual gating as shown in *Online Supplementary Figure S1* for B cells and PC with subsequent cluster exploration to analyze mean fluorescence intensity (MFI) values across each cellular subset. A more detailed description can be found in the *Online Supplementary Appendix*.

CPC were identified by a $CD45^{-}CD38^{high}$ immunophenotype. CD56 expression was subsequently used to identify aberrant CPC (i.e., $CD56^{+}$ CTPC), as CD56 represents one of the most consistently altered markers in clonal plasma cells.[15] Light chain clonality (κ/λ) and additional markers included in the EuroFlow next-generation flow cytometry (NGF) panel, such as CD27 or CD81, were not

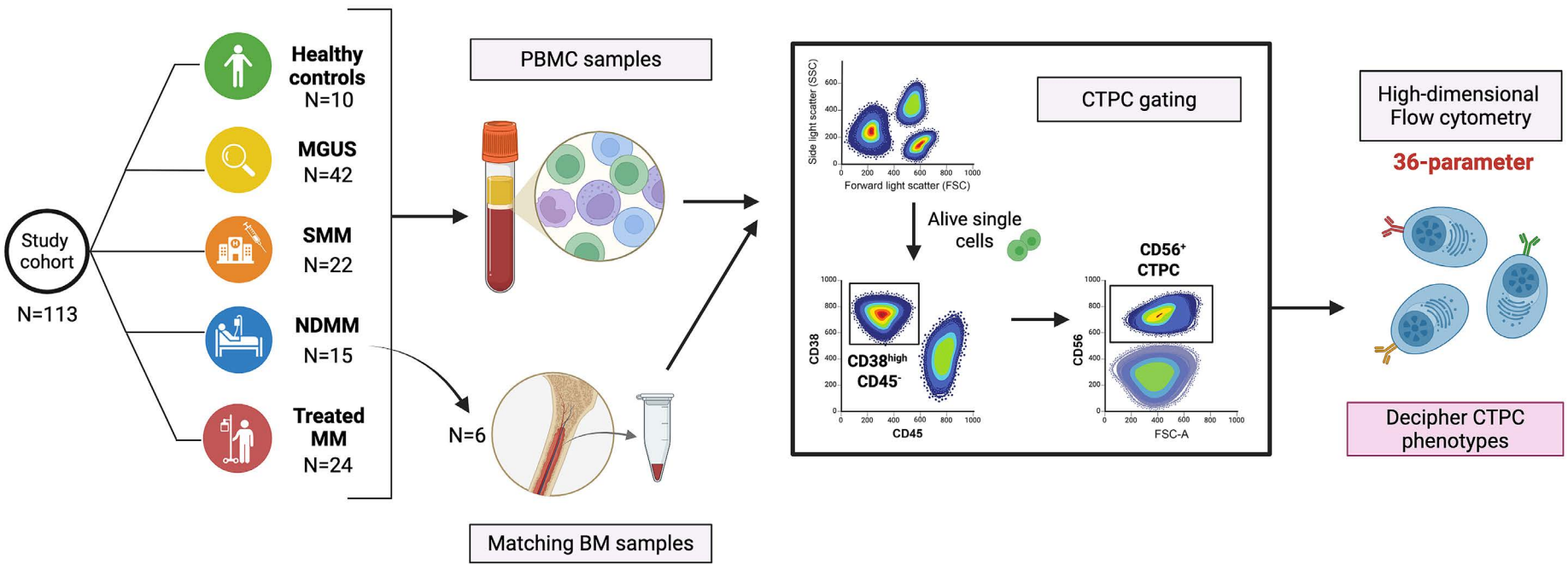


Figure 1. Overview of study design and samples. The study included 5 cohorts: healthy individuals, monoclonal gammopathy of undetermined significance (MGUS), smouldering multiple myeloma (SMM), newly diagnosed MM (NDMM), and treated MM. Peripheral blood mononuclear cells (PBMC) were collected from all participants, and 6 additional matched bone marrow (BM) aspirates were obtained. After quality control, samples were analyzed by multi-dimensional spectral flow cytometry to characterize CD56+ circulating tumor plasma cell (CTPC) phenotypes. Created with: Stanger, A. [2026] https://BioRender.com/xn04d8n).

Table 1. Clinical, laboratory and molecular characteristics of the study cohort.

Characteristics	MGUS N=42	SMM N=22	NDMM N=5	treated MM N=24	Healthy controls* N=10
Sex: male, N (%)	20 (48)	9 (41)	7 (47)	13 (54)	NA
Age initial diagnosis, years, mean (range)	57.7 (33-86)	61.3 (35-79)	67.1 (41-87)	61.3 (43-81)	NA
Age at sampling, years, mean (range) <65 ≥65	62.8 25 17	65.9 10 12	67.1 5 10	66.3 11 13	NA
Hemoglobin level, mean, g/dL (range) Unknown, N	13.6 (10.1-15.8) 5	13.4 (10.2-15) 0	11.6 (8.2-15.5) 0	12.4 (8.9-16.3) 0	NA
B2-microglobulin, median, mg/L (range) >5.5, N (%) >5.5 & creatine <1.2 mg/dL, N (%) Unknown, N (%)	2.3 (1.1-4.5) 0 (0) 0 (0) 11 (26)	2.3 (1.4-3.3) 0 (0) 0 (0) 2 (9)	3.8 (1.5-7.1) 2 (13) 1 (7) 0 (0)	5.5 (1.8-17.5) 6 (25) 2 (8) 2 (8)	NA
ISS, N (%) 1 2 3 Unknown	NA	NA	4 (27) 7 (47) 4 (27) 0 (0)	5 (21) 11 (46) 8 (33) 0 (0)	NA
IMS/IMWG-HR consensus 2025, N (%) Standard-risk High-risk Unknown	NA	NA	11 (73) 3 (20) 1 (7)	15 (62) 4 (17) 5 (21)	NA
MGUS risk score, N (%) 0 low 1 intermediate-low 2 intermediate-high 3 high	16 (38) 20 (48) 5 (12) 1 (2)	NA	NA	NA	NA
SMM 20/2/20 risk score, N 0 low 1 intermediate ≥2 high	NA	7 7 8	NA	NA	NA
Immunoglobulin subtype, N (%) IgG IgA LCO IgM	33 (78) 4 (10) 1 (2) 4 (10)	16 (73) 5 (23) 1 (4.5) 0 (0)	10 (67) 4 (27) 1 (7) 0 (0)	13 (54) 6 (25) 5 (21) 0 (0)	NA
Induction treatment, N (%) PI IMiD PI + IMiD Other	NA	NA	NA	6 (25) 3 (13) 15 (62) 0 (0)	NA
HD/ASCT, N (%) No HD/ASCT Single HD/ASCT Tandem HD/ASCT	NA	NA	NA	7 (29) 12 (50) 5 (21)	NA
Treatment at sampling, N (%) IMiD Anti-CD38 Anti-CD38 + IMiD Anti-BCMA CAR T Watch and wait	NA	NA	NA	19 (79) 0 (0) 0 (0) 1 (4) 4 (17)	NA
Remission at sampling, N (%) CR PR PD	NA	NA	initial diagnosis	17 (71) 4 (17) 3 (12)	NA

*Samples were obtained from a blood bank and were fully anonymized. MGUS: monoclonal gammopathy of undetermined significance; SMM: smouldering multiple myeloma; NDMM: newly diagnosed multiple myeloma; ISS: International Staging System; IMS: International Myeloma So-

Continued on following page.

ciety; HR: hygh-risk; HD/ASCT: high-dose chemo-therapy/autologous stem cell transplantation; CR: complete response; PR: partial response; PD: progressive disease; IMWG: International Myeloma Working Group; PI: proteasome inhibitor; IMiD: immunomodulatory drug; NA: not applicable; LCO: light chain only; N: number; BCMA: B-cell maturation antigen; CAR: chimeric antigen receptor.

primarily used to gate CTPC. The limit of detection was set at >20 CPC events, and samples below this threshold were excluded from marker expression analyses.

Ethics and informed consent

The study was approved by the institutional Ethical Committees in accordance with the Declaration of Helsinki (number 161/2022B02). All patients and controls provided informed consent before study inclusion.

Statistical analysis

Statistical analyses were performed using GraphPad Prism (v10.5.0). Comparisons were performed after analysis of normal distribution using the Anderson-Darling test. Continuous variables were analyzed using Welch's *t* test, paired *t* test, Mann-Whitney test or Wilcoxon rank-sum tests as appropriate. We performed ANOVA (normally distributed) or Kruskal-Wallis (K-W, non-parametric) to investigate differences in >2 groups, with adjustment for multiple comparisons by *post hoc* Benjamini, Krieger and Yekutieli procedure for false discovery rate (FDR) correction. Desired FDR Q was set at 0.05. Test-specific effect sizes were reported for all analyses, with 95% confidence intervals (CI) where applicable. All tests were two-sided, and *P* values <0.05 were considered significant. In case of FDR correction, adjusted *P* values (q values) of <0.05 were considered a statistically significant discovery.

Results

Patient and treatment characteristics

One hundred and three patients were included in the analysis, of which 42 (40.7%) had MGUS, 22 (21.4%) SMM, 15 (14.6%) NDMM and 24 (23.3%) treated MM at sample collection (Figure 1). In addition to PBMC, paired BM samples were available for six of 15 NDMM patients (40.0%). Clinical baseline and treatment characteristics are summarized in Table 1. Mean interval from initial diagnosis to sample collection was 60.2 months (interquartile range [IQR], 13.8-78.3) for MGUS, 53.0 months (IQR, 14.0-89.3) for SMM, 1.0 month (IQR, 0.0-1.0) for NDMM and 60.0 months for treated MM (IQR, 36.3-77.3). All subsequent results are presented with reference to PBMC unless otherwise specified and focus on differences between MGUS, SMM and NDMM in comparison to healthy controls.

B-cell counts and disease progression

The percentage of total B cells ($CD19^+$) of all $CD45^+$ cells in PB did not significantly differ between healthy controls (mean 10.43%, standard deviation [SD] 2.20), MGUS (mean 10.77%, SD 4.45), SMM (mean 9.93%, SD 5.64) and NDMM (11.27%, SD 7.01). However, a relevant subset of MGUS (33%), SMM (50%) and MM patients (40%) had reduced B-cell proportions compared to healthy controls (Figure 2A). Moreover, subset analysis revealed distinct

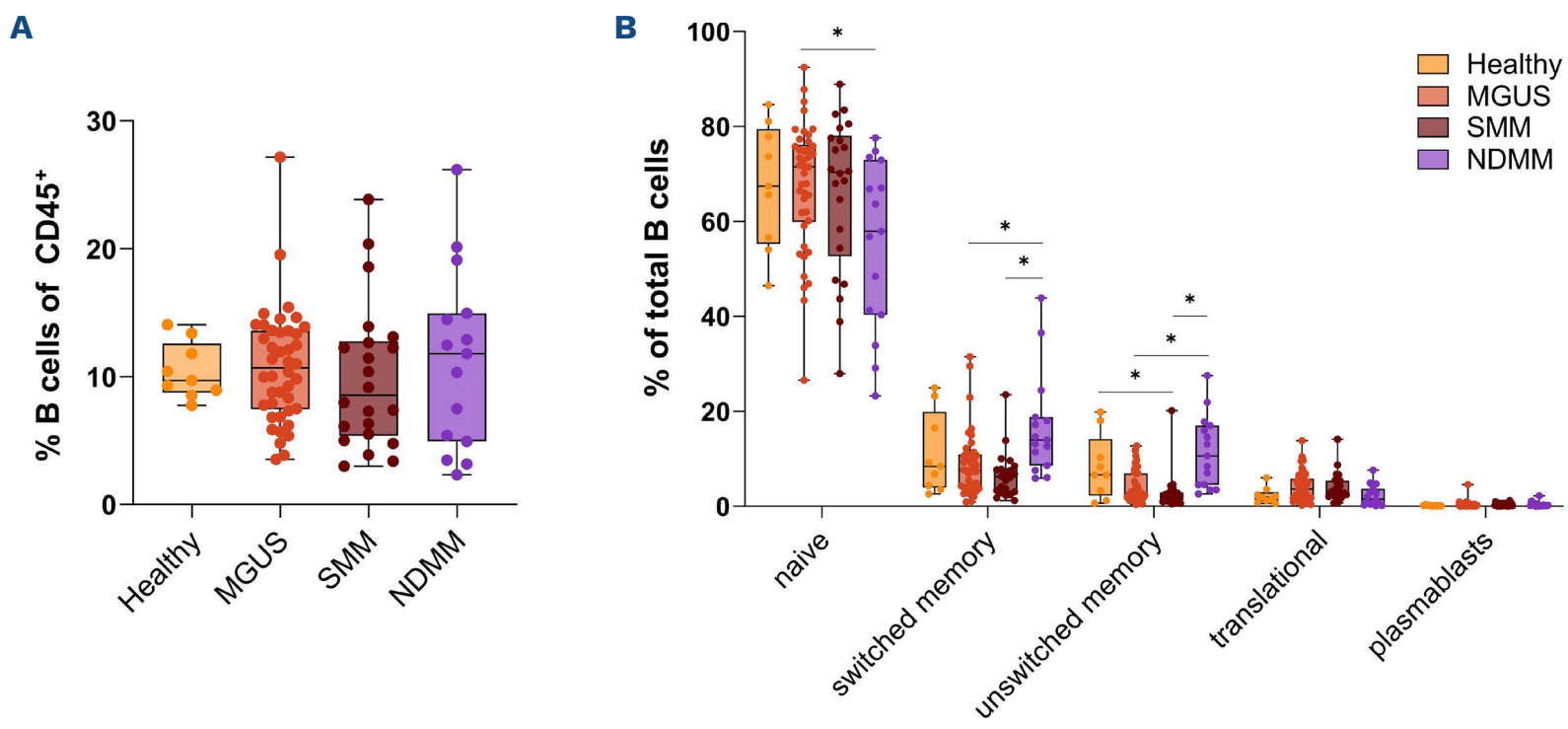


Figure 2. Distribution of B-cell subsets in peripheral blood changes with disease evolution. (A) Proportion of B cells ($CD19^+$) among $CD45^+$ peripheral blood cells for each group; healthy N=9; monoclonal gammopathy of undetermined significance (MGUS) N=42; smouldering multiple myeloma (SMM) N=22; newly diagnosed MM (NDMM) N=15. Whiskers mark minimum and maximum. (B) Distribution of B-cell subsets according to disease stage. Values are shown as percentage of total B cells in peripheral blood. Statistical significance was determined via ANOVA or Kruskal-Wallis with *post hoc* false discovery rate correction. Asterisks mark a statistically significant discovery.

changes in the composition of the B-cell compartment with disease progression. The percentage of naive B cells in MGUS (67.65%) and SMM (65.94%) did not differ from healthy controls (67.46%) (healthy *vs*. MGUS adj. *P*=0.851; healthy *vs*. SMM adj. *P*=0.837), whereas a marked drop in naive B cells was seen in NDMM (55.16%) compared to MGUS (adj. *P*=0.036; Hedges' g=0.84; 95% CI: 0.21-1.46) and SMM (adj. *P*=0.089; Hedges' g=0.63; 95% CI: 0.02-1.24) (Figure 2B). Switched and unswitched memory B cells were lower in MGUS (8.79% and 4.08%, respectively) and SMM (6.58% and 2.92%, respectively) compared to healthy levels (11.07% and 8.31%; healthy *vs*. SMM adj. *P*=0.013 for unswitched, r_{rb}=0.41) but significantly higher in NDMM (16.84% and 11.50%; NDMM *vs*. MGUS adj. *P*=0.004; r_{rb}=0.43 and NDMM *vs*. SMM adj. *P*<0.001, r_{rb}=0.61 for switched; NDMM *vs*. MGUS adj. *P*< 0.001, r_{rb}=0.53 and NDMM *vs*. SMM adj. *P*<0.001; r_{rb}=0.71 for unswitched) (Figure 2B). Conversely, a trend toward higher levels of translational B cells in MGUS (4.15%) and SMM (4.04%) was seen compared to NDMM (2.21%), yet this trend did not reach statistical significance (NDMM *vs*. MGUS/SMM both *P*=0.065). No differences were found for plasmablast counts in PB (Figure 2B).

Circulating plasma cell and circulating tumor plasma cell counts and disease progression

CD56$^-$ CPC could be found in 100% of healthy donors with a median of 44.6/100.000 cells. They were slightly lower in MGUS (median 37.2/100.000 cells) and SMM (37.7/100.000 cells) but comparable to healthy levels in NDMM (median 48.7/100.000 cells) (Figure 3A). The median number of CD56$^+$ CTPC rose significantly from MGUS (2.54; IQR, 1.13-7.18) to SMM (6.96; IQR, 2.66-13.89) to NDMM (median 16.34; IQR, 12.86- 86.78) (overall *P*<0.001; ε^2= 0.17) (Figure 3B). For the whole CPC compartment in the PB, this translated into a significantly increased median percentage of CD56$^+$ CTPC from MGUS (5.62%), to SMM (13.01%) and NDMM (32.41%) (overall *P*=0.002; ε^2=0.20) (Figure 3C). PC with aberrant CD56 expression were also found in healthy donors, albeit at lower frequencies compared to precursor states and NDMM (median 1.9/100.000 cells; IQR, 0.49-3.84, median percentage of all CPC 3.65%) (Figure 3B, C).

Exploratorily, we categorized all samples into "CTPC high" (≥0.02%) and "CTPC low" (<0.02%) by using a threshold established by Kostopoulos *et al.*[16] for CTPC enumeration by NGF. Classified as "CTPC high" were 9.5% (4/42) of MGUS, 18.2% (4/22) of SMM and 40.0% (6/15) of NDMM (Figure 3D).

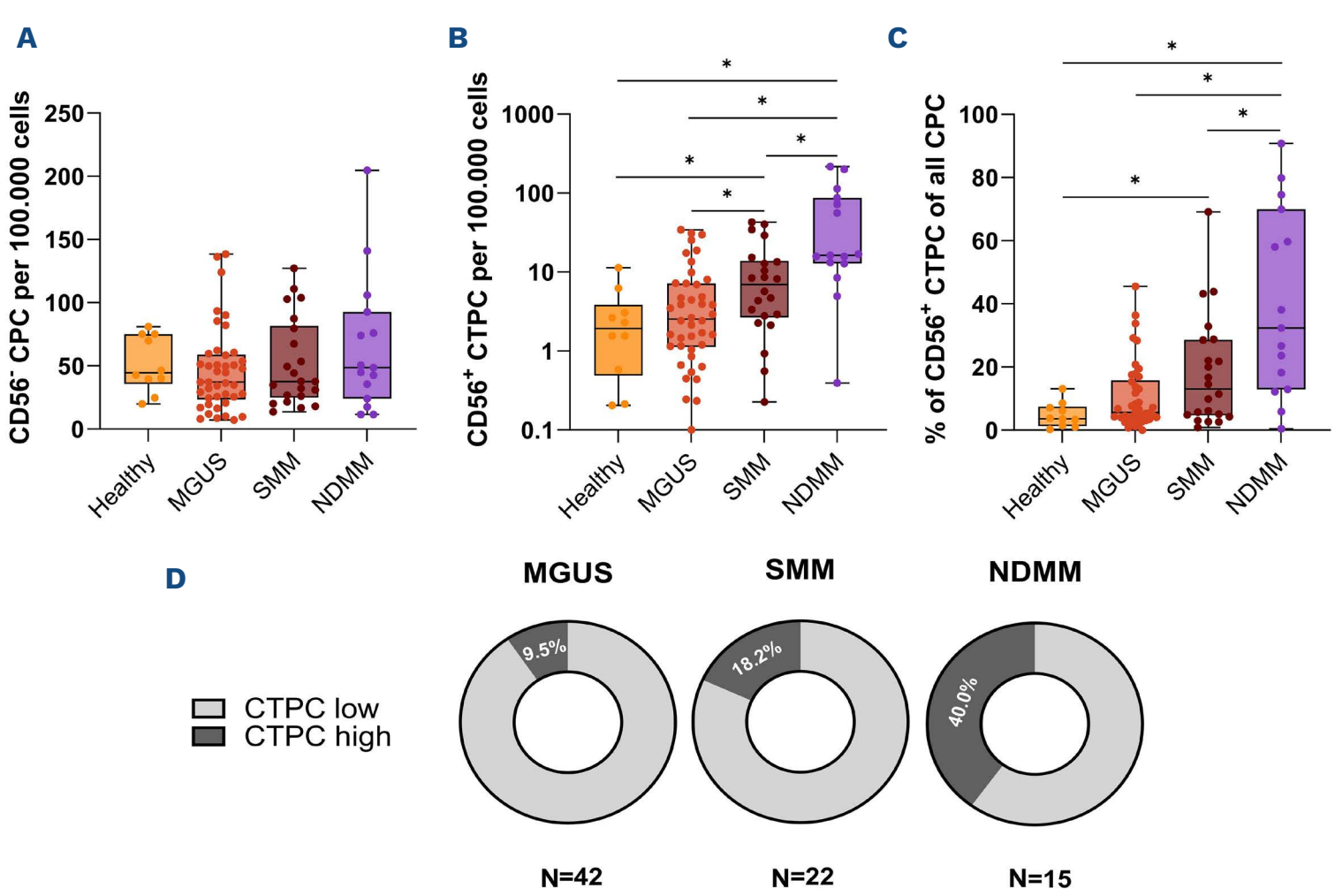


Figure 3. CD56$^+$ circulating tumor plasma cell counts discriminate disease stage. (A) Relative distribution of CD56$^-$ circulating plasma cells (CPC) (CD45$^-$ CD38$^+$ CD56$^-$) for each group; healthy N=10, monoclonal gammopathy of undetermined significance (MGUS) N=42, smouldering multiple myeloma (SMM) N=22, newly diagnosed MM (NDMM) N=15. (B) Relative distribution of CD56$^+$ circulating tumor PC (CTPC, CD45$^-$ CD38$^+$ CD56$^+$) for each group. (C) Percentage of CD56$^+$ CTPC from all CPC for each group. Data is presented as box-and-whisker plot with median values indicated. Statistical significance was determined via Welch's ANOVA with *post hoc* false discovery rate correction. Asterisks mark a statistically significant discovery. (D) Visualization of the distribution of „CTPC high" samples (≥0.02% CD56$^+$ CTPC of all nucleated cells in peripheral blood) *versus* „CTPC low" samples (<0.02% CD56$^+$ CTPC) at different disease stages.

Acknowledging the cohort size in our study as well as the use of a SFC, we did not observe any clear correlations between "CTPC high" and advanced risk scores for MGUS and SMM cases. Among the six NDMM samples classified as "CTPC high", two patients were also classified as IMS/IMWG high-risk (33.3%). All "CTPC low" NDMM samples had standard-risk according to IMS/IMWG criteria, except one classified as high-risk due to elevated β2-microglobulin with additional gain1q21. When applying a less stringent threshold of 2% of nucleated cells for classification as "CTPC high", none of the patients in our groups met this criterion.

Circulating tumor plasma cell phenotype profiles

CTPC phenotypic profiling was based using a total of 36 parameters (*Online Supplementary Table S1*), with CTPC phenotypically defined as $CD45^{-}CD38^{high}CD56^{+}$ events, whilst clonality was not assessed. Therefore, the findings reflect the $CD56^{+}$ CTPC-like subset. CPC from healthy controls served as comparison. Across disease progression from MGUS and SMM to NDMM, $CD56^{+}$ CTPC showed distinct changes in marker expression, including aberrant expression of markers not typically expected with the CTPC phenotype. All *P* values for each marker and comparison are provided in *Online Supplementary Table S2*, and boxplots for each marker are shown in *Online Supplementary Figure S2*.

B- and plasma-cell related markers on circulating tumor plasma cells across disease stages

Consistent with normal PC maturation, $CD56^{+}$ CTPC showed increasing CD38 expression accompanied by loss of CD19 expression across disease stages, reaching the highest CD38 levels (according to its mean fluorescence intensity [MFI]) in NDMM. CD27 levels were consistently lower compared to healthy PC. CD138 and BCMA expression remained stable across MGUS, SMM, and NDMM, whereas CD307e was significantly upregulated in SMM and NDMM compared to MGUS (both adj. $P<0.01$; $r_{rb}=0.34$ and 0.59) (Figure 4A). Although, particularly in MGUS, wide interpatient variability was observed. CD20 showed no clear pattern across stages; however, the highest levels in NDMM were observed in a patient with t(11;14). Interestingly, even though CTPC were defined as CD45 negative, the CD45RA isoform showed robust expression in MGUS, whereas levels were lowest in NDMM (overall $P<0.001$; $\eta^2=0.41$; 95 % CI: 0.23-0.55) (Figure 4B, G; *Online Supplementary Figure S4*).

T- and myeloid-cell related markers on circulating tumor plasma cells across disease stages

While CD3 expression on PC was mutually exclusive with CD56 in our data, resulting in the absence of $CD3^{+}$ CTPC (*data not shown)*, several T-cell associated markers were aberrantly expressed on $CD56^{+}$ CTPC despite the lack of CD3 expression. CD4 expression declined in MGUS samples but showed no further significant changes in SMM and NDMM relative to healthy PC. In contrast, CD8 expression on CTPC seemed to robustly increase from precursor states to NDMM (overall $P<0.001$; $\varepsilon^2=0.36$) (Figure 4C). In cross-sectional comparison, expression of the interleukin (IL) receptor subunits CD25/IL-2RA and CD123/IL-3RA were lower in MGUS and SMM than in healthy controls, but again equally expressed in NDMM (CD25: overall $P<0.001$; $\varepsilon^2=0.22$; CD123: overall $P<0.001$; $\varepsilon^2=0.29$) (Figure 4D, H). In contrast to IL receptor subunits, the myeloid-related cell markers CD14 and CD16 were highest expressed on $CD56^{+}$ CTPC in MGUS, followed by a lower expression across subsequent disease stages (CD14: overall $P=0.010$; $\varepsilon^2=0.10$; CD16: overall $P=0.001$; $\varepsilon^2= 0.15$) (Figure 4D).

Activation, checkpoint, and chemokine receptor signatures on circulating tumor plasma cells across disease stages

We next assessed aberrant expression of activation signatures on $CD56^{+}$ CTPC. The activation marker CD69 showed declining levels from MGUS over SMM to NDMM samples, with the lowest MFI observed in NDMM (overall $P<0.001$; $\varepsilon^2=0.34$) (Figure 4E). In contrast, HLA-DR and HLA-ABC expression, reduced in MGUS and SMM, reached levels comparable to those in healthy controls in NDMM (Figure 4B). Among checkpoint molecules, TIM-3 expression on $CD56^{+}$ CTPC showed a trend toward upregulation in NDMM compared to MGUS and SMM, although this did not reach statistical significance (NDMM *vs*. MGUS/SMM: both adj. $P=0.103$; $r_{rb}=0.17$ and 0.38), whereas PD-1 and TIGIT showed the opposite pattern, with significant lower expression in SMM and NDMM (NDMM *vs*. MGUS: adj. $P<0.001$ for PD-1; $r_{rb}=0.59$; $P=0.002$ for TIGIT; $r_{rb}=0.48$) (Figure 4E, I).
Interestingly, the chemokine receptors CCR6 and CCR7 were elevated in NDMM compared to all other groups, with CCR7 showing a particularly pronounced increase (CCR6: NDMM *vs*. MGUS/SMM adj. $P<0.01$; $r_{rb}=0.39$ and 0.50; CCR7: NDMM *vs*. MGUS/SMM adj. $P<0.001$; $r_{rb}=0.60$ and 0.67) (Figure 4F, J). The expression of CCR4 remained stable across disease stages and was comparable to MFI on CPC from healthy donors.

Circulating tumor plasma cell phenotypes in the treated multiple myeloma cohort

In the treated MM cohort (N=24), a mostly reversed pattern compared to the disease evolution from MGUS, SMM to NDMM could be observed. Compared to NDMM, $CD56^{+}$ CTPC displayed a significant lower expression of CD38 ($P<0.001$; $r_{rb}=0.73$) and CD56 ($P=0.001$; $r_{rb}=0.62$) as well as a significant regain of CD19 ($P=0.006$; $r_{rb}=0.52$) and CD45RA ($P<0.001$; Hedges' g=1.79; 95% CI: 1.05-2.58) after treatment (Figure 5A-C). Interestingly, CD307e expression was significantly lower in the treated cohort ($P<0.001$; $r_{rb}=0.76$), whereas the expression of BCMA increased compared to NDMM ($P=0.020$; Hedges' g=0.67; 95% CI: 0.02-1.35) (Figure 5B). Of note, only one of our treated patients received

BCMA-directed therapy (Table 1) and this patient did show a comparable BCMA expression to other samples without BCMA-directed therapy.

The MFI of T-cell related markers such as CD4 and CD8 significantly decreased post-treatment compared to NDMM (P<0.001; Hedges' g=1.02; 95% CI: 0.34-1.72; and P<0.001; Hedges' g=1.52; 95% CI: 0.81-2.28, respectively). Moreover, the expression of the IL receptor subunits CD25 (P<0.001; r_{rb}=0.81) and CD123 (P=0.003; Hedges' g=0.93; 95% CI: 0.26-1.62) was significantly lower in the treated cohort compared to NDMM (Figure 5D). Checkpoint and chemokine receptor expression appeared to recover after treatment. Although based on a cross-sectional setting, the trends were striking, with PD-1 (P<0.001; r_{rb}=0.78) and TIGIT (P=0.003; r_{rb}=0.56) increasing and TIM-3 (P=0.002; r_{rb}=0.78), CCR6 (P=0.192; r_{rb}=0.26) and CCR7 (P=0.004; r_{rb}=0.55) decreasing again compared to NDMM (Figure 5E, F).

Circulating tumor plasma cell phenotypes compared to bone marrow plasma cell phenotypes in newly diagnosed multiple myeloma

For six patients with NDMM paired PB and BM samples were available, which were further analyzed regarding phenotypic differences. The six combined samples presented with similar differences when comparing PB and BM (*Online Supplementary Figure S3*). Whereas CD69 expression was low on CD56$^+$ CTPC in NDMM, BMPC exhibited markedly higher CD69 levels (P=0.013; d_z=1.55; 95% CI: 0.68-4.16), potentially in analogy to its role in tissue residency in T cells (Figure 6A). Conversely, CD56$^+$ CTPC showed a significantly higher expression of CD138 (Figure 6A) than their BM counterparts (P=0.002; d_z=2.48; 95% CI: 0.77-4.15), whereas expression of

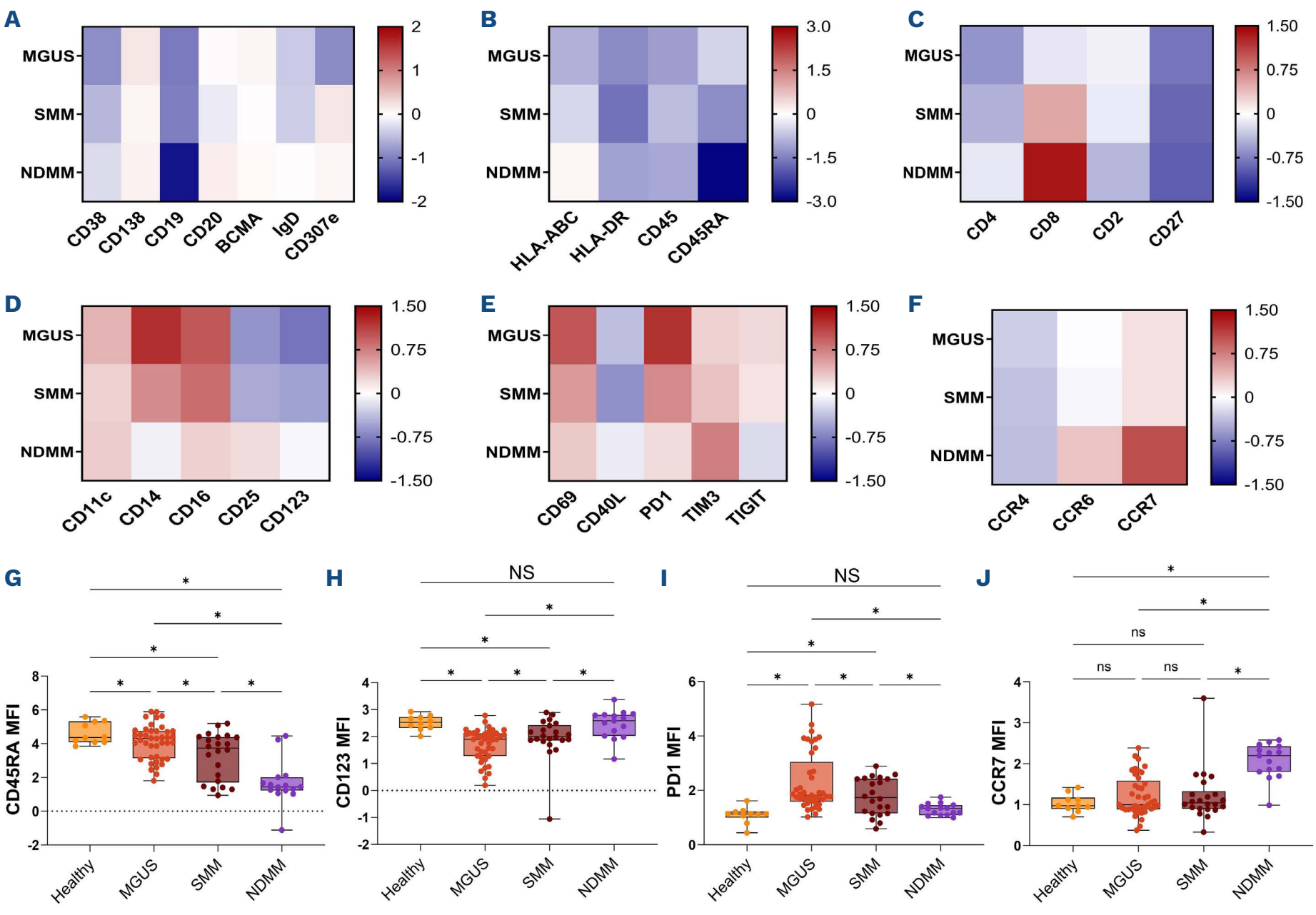


Figure 4. CD56$^+$ circulating tumor plasma cells show phenotypic evolution and expression of atypical markers with disease progression. (A-F) Expression of surface markers within the CD56$^+$ circulating tumor plasma cell (CTPC) population at different disease stages, displayed as heatmap; monoclonal gammopathy of undetermined significance (MGUS) N=41, smouldering multiple myeloma (SMM) N=22, newly diagnosed MM (NDMM) N=15. Values are shown as change in the group's mean fluorescence intensity (MFI) compared to the MFI of the healthy control group (N=10). Circulating plasma cells (CPC) were used as control in the healthy cohort. (G-J) Transformed MFI values on CD56$^+$ CTPC at different disease stages for CD45RA, CD123, PD1 and CCR7 in comparison to CPC from the healthy cohort. Data is presented as box and whisker plots with median values indicated. Statistical significance was determined via ANOVA or Kruskal-Wallis with *post hoc* false discovery rate correction. Asterisks mark a statistically significant discovery; NS: no statistically significant discovery.

CD14 (P=0.007; d_z=1.77; 95% CI: 0.42-3.08), CD25 (P=0.009; d_z=1.67; 95% CI: 0.77-4.45) and CD123 (P=0.017; d_z=1.44; 95% CI: 0.59-3.93) (Figure 6A, B; *Online Supplementary Figure S3*) was significantly lower on CD56$^+$ CTPC. Interestingly, BCMA and, in particular, CD307e expression were significantly higher on BMPC than on CD56$^+$ CTPC (P=0.049; d_z=1.06; 95% CI: 0.01-2.05; and P=0.002; d_z=2.53; 95% CI: 1.37-6.48, respectively) (Figure 6C). CD8 showed a markedly higher expression on BMPC compared to CD56$^+$ CTPC in all samples (P=0.002; d_z=2.38; 95% CI: 1.29-6.10) (Figure 6B). Finally, CCR6 was significantly lower expressed on CD56$^+$ CTPC than on BMPC (P=0.037; d_z=1.15; 95% CI: 0.06-2.18), whereas no differences were observed for CCR4 and CCR7, possibly reflecting the distinct chemokine milieu in PB (Figure 6D).

Discussion

In this study, we used multi-dimensional spectral flow cytometry with a 33-marker (36 parameter) panel in a cohort of MGUS, SMM, NDMM, and treated MM patients to delineate B-cell and CD56$^+$ CTPC phenotypes across disease stages and after treatment.

Using this technique, we showed no significant differences regarding absolute B-cell counts and subset distributions in PB between MGUS patients and healthy controls. However, NDMM samples were marked by higher levels of switched and unswitched memory B cells compared to precursor stages as well as a drop in naive B-cell counts. The observation of increased memory B cells is consistent with previous studies,[17,18] and has led to speculation about possible "myeloma-initiating" or MM stem cells among the circulating memory B-cell population.[18,19] Furthermore, it has been shown that MM cells in relapse seem to emerge from a pool of progenitor cells found among B cells,[20] highlighting the necessity of further investigation into the relationship between B cells and MM cells.

Analyses of relative and absolute CD56$^+$ CTPC counts demonstrated stepwise increases from MGUS to SMM to NDMM, as reported before.[21] After exploratorily classifying all samples into "CTPC high" (≥0.02%) and "CTPC low" (<0.02%) by using a binary threshold analogous to Kostopoulos *et al.*,[16] we did not observe strong overlap with established risk stratification models in precursor stages. For NDMM, virtually all CTPC-low cases (8/9, 89%) were classified as standard risk by the updated IMS/IMWG HR guidelines. Interestingly, a gain or amplification of 1q21 was present in four of six (66.7%) CTPC-high samples, but only in two of

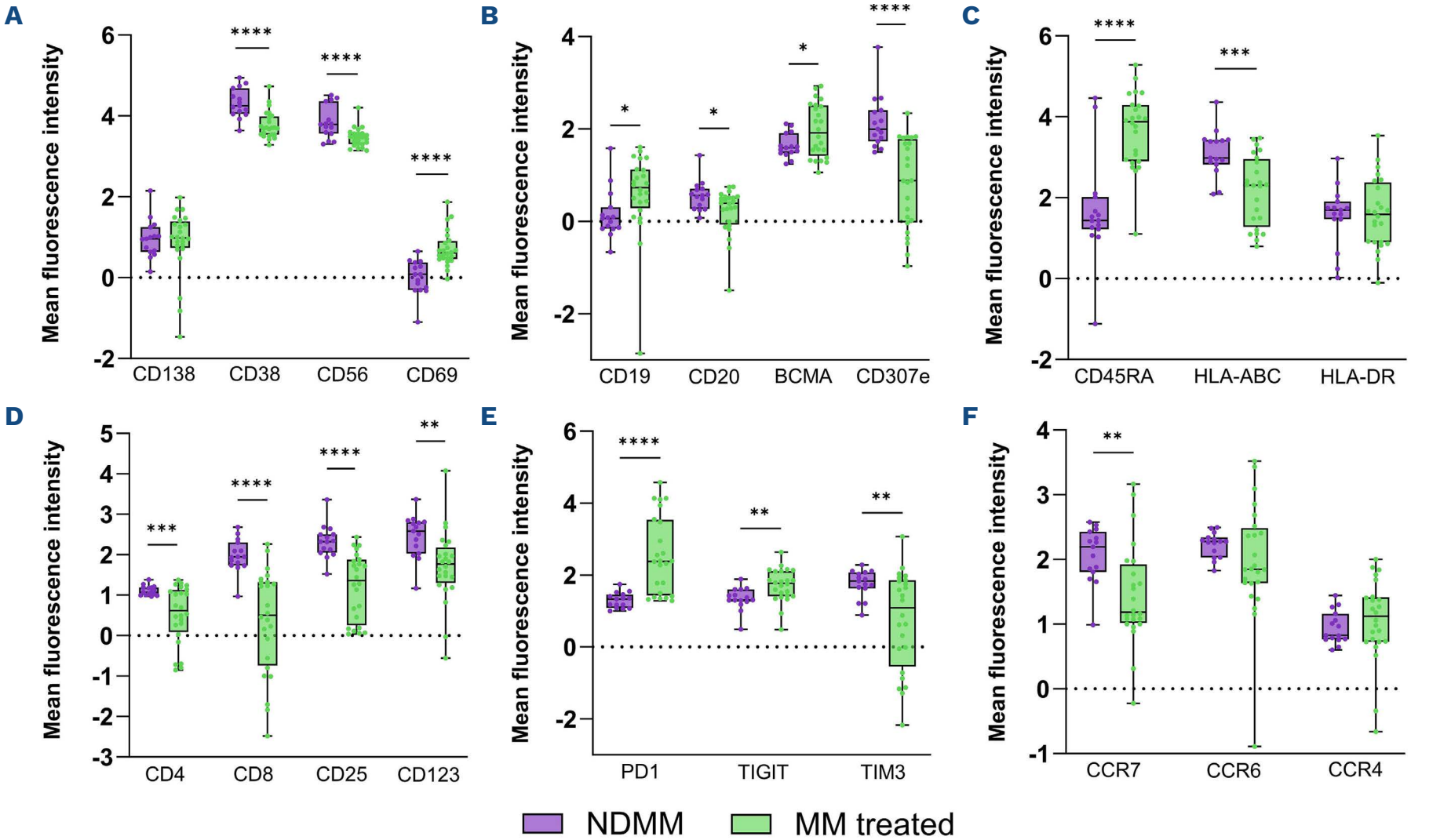


Figure 5. Comparison of expression patterns on CD56$^+$ circulating tumor plasma cells in untreated and treated multiple myeloma. (A-F) Transformed mean fluorescence intensity values of selected markers on CD56$^+$ circulating tumor plasma cells (CTPC) in treated and untreated multiple myeloma (MM); newly diagnosed MM (NDMM) N=15, treated MM N=24. Data is presented as box and whisker plots with median values indicated. Statistical significance was determined via Welch's *t* test (for normally distributed data) or Mann-Whitney test (for non-parametric data). *P<0.05; **P<0.01; ***P<0.001; ****P≤0.0001.

nine (22.2%) CTPC-low samples. This observation confirms a trend priorly seen for CTPC in AL amyloidosis.[22] However, comparisons with risk models remain underpowered due to cohort size and may not be directly transferable due to different gating strategies.

The CD56$^+$ CTPC phenotypes showed maturation-consistent changes across disease stages in B-cell and PC markers. This was surprisingly accompanied by acquisition of various T-cell and myeloid-related features not typically associated with CPC. Notably, NDMM samples could be well distinguished from healthy controls, MGUS and SMM by several specific expression patterns. First, they showed a more terminally differentiated and malignant PC phenotype than MGUS and SMM samples. CD38 and CD56 expressions were highest, while CD19, CD27, and CD45RA were lower expressed. Interestingly, CD20 expression was highest in NDMM with t(11;14), consistent with this translocation being associated with a more B-cell-like phenotype.[23] Second, the antigen presentation machinery via HLA-ABC and HLA-DR appeared to be altered in NDMM. HLA-ABC, reduced in MGUS and SMM, reached comparable high levels to healthy controls, potentially pointing to an advanced tumor stage with activated immune microenvironment as it is seen in breast cancer cells expressing HLA-ABC.[24] Third, non-canonical markers expressed on CTPC suggest a potentially modified checkpoint and survival-signaling profile in NDMM. Specifically, PD-1 and TIGIT were lower, but TIM-3 levels were higher on NDMM CD56$^+$ CTPC compared to MGUS and SMM samples. Given its inhibitory role known from tumor-infiltrating lymphocytes,[25] elevated TIM-3 expression on CTPC warrants future functional validation to determine whether TIM-3 plays a biological role in CTPC persistence in PB. Furthermore, several IL receptor subunits (CD25/IL-2RA, CD123/IL-3RA) were lower on CTPC in MGUS and SMM than in healthy controls but higher in NDMM. Among others, they activate STAT5, which has been linked to suppression of anti-tumor immunity and enhanced tumor cell survival.[26] This pattern would be consistent with increased cytokine responsiveness and pro-survival signaling in advanced MM disease.[27] Compared with BMPC, CD25 and CD123 were lower on CD56$^+$ CTPC (both P<0.01), possibly suggesting niche-specific survival programs. In line with our findings, the BM of MM patients has been shown to be enriched for IL-3 and interactions between plasmacytoid dendritic cells and BMPC might further support this signalling axis.[28,29] As our panel identified CTPC without clonality assessment, we acknowledge that non-canonical marker patterns may also occur on reactive, polyclonal PC that transiently express CD56.

Notably, CCR6 and CCR7 were significantly elevated on CD56$^+$ CTPC in NDMM compared to all other groups, suggesting potential differences in trafficking cues. CCR6 was even higher expressed on BMPC than on matched CD56$^+$ CTPC (P=0.037), in line with reports that malignant PC upregulate CCR6 in their TME and promote osteolytic bone disease.[30] This modified chemokine signature could relate to extramedullary disease (EMD), as a correlation between CCR7 expression on BMPC and EMD has already

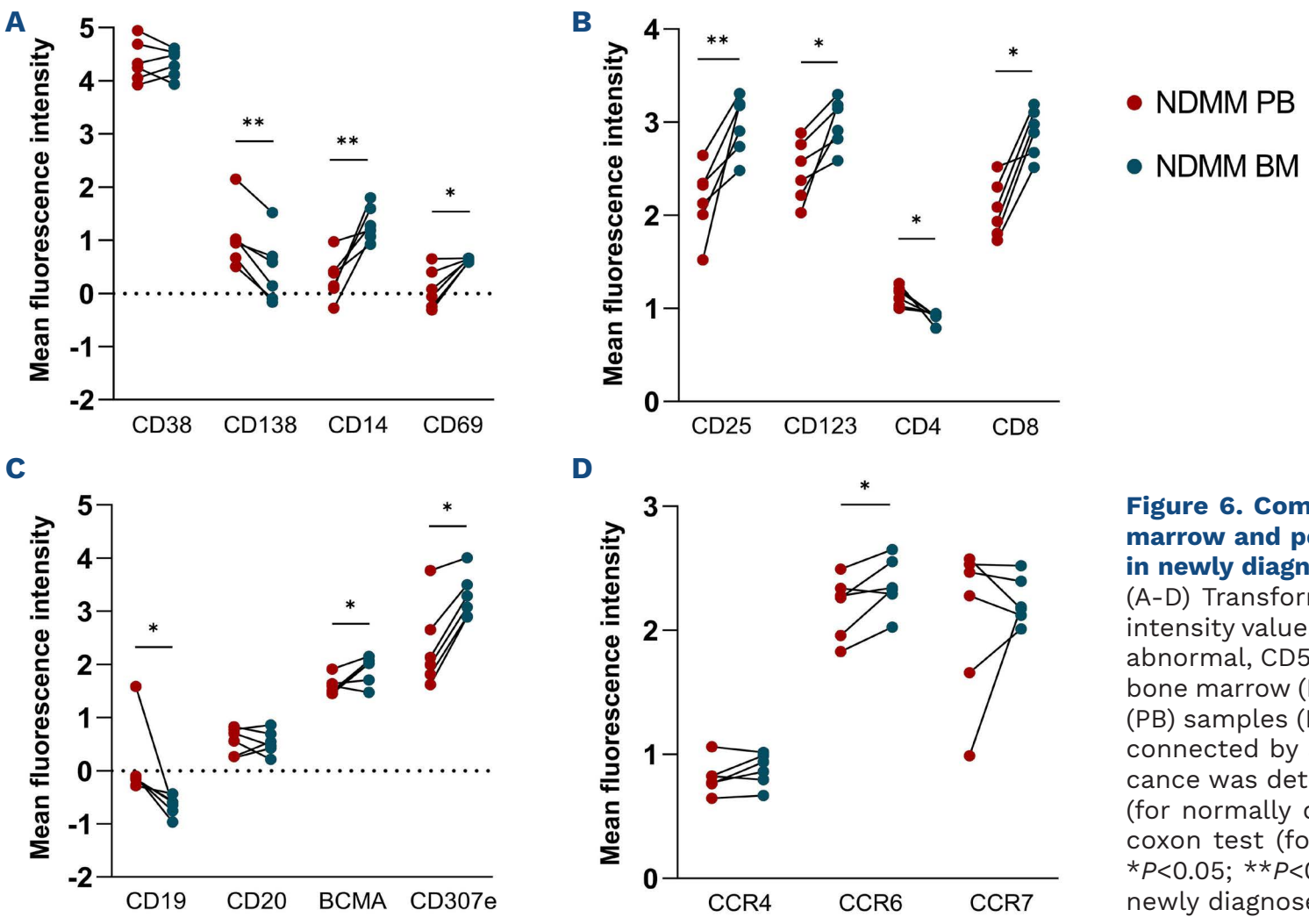


Figure 6. Comparison of paired bone marrow and peripheral blood samples in newly diagnosed multiple myeloma. (A-D) Transformed mean fluorescence intensity values of selected markers on abnormal, CD56$^+$ plasma cells in paired bone marrow (BM) and peripheral blood (PB) samples (N=6). Paired samples are connected by a line. Statistical significance was determined via paired *t* test (for normally distributed data) or Wilcoxon test (for non-parametric data). *P<0.05; **P<0.01; ***P<0.001. NDMM: newly diagnosed multiple myeloma.

been shown.[31] Unfortunately, our cohort contained too few patients with EMD at sampling to draw a robust connection. Lastly, the activation marker CD69 was lower in NDMM samples, potentially in analogy to its role in tissue residency in memory T cells.[32] This aligns with higher CD69 levels on BMPC than on matched CTPC.

In the treated MM cohort, the described NDMM-associated phenotypic changes were partially or fully normalized. The significant lower CD38 expression post-treatment may reflect either disease remission or antigen escape secondary to anti-CD38 therapy.[33] Moreover, the higher expression of CD19 post treatment could represent the accumulation of less-differentiated PC subclones after therapy-induced pressure.[34]

Given their therapeutic relevance, we assessed BCMA and CD307e expression across disease stages. BCMA on CD56$^+$ CTPC did not differ meaningfully between MGUS, SMM, and NDMM, with slightly higher levels after treatment. This finding was unlikely to be influenced by BCMA-directed therapies in our cohort, as only one patient had received anti-BCMA chimeric antigen receptor (CAR) T cells. In the six paired NDMM samples, BCMA expression was higher on BMPC than on CD56$^+$ CTPC (P=0.049). CD307e was significantly increased in SMM and NDMM compared to MGUS (both P<0.01) and was also higher on BMPC than on CD56$^+$ CTPC (P=0.002). The pronounced expression in SMM samples may warrant evaluation as a therapeutic target specifically in this precursor state, however, validation in larger cohorts is essential.

Limitations of this study include the cross-sectional design and limited per-group sample sizes, particularly for matched BM samples. Although PBMC sample numbers are decent, statistical power was limited to detect robust associations with clinical features, considering also inter-patient variability in marker expression. Moreover, our CTPC gating strategy relied on CD56 expression to identify aberrant CPC. While this approach captures the predominant malignant phenotype reported for CTPC in MM, it likely underestimates the full CTPC compartment and may include rare non-clonal plasma cells due to non-assessed clonality. Future studies with larger, longitudinal cohorts, CTPC gating as defined in the full EuroFlow NGF panel, and functional validation will be mandatory to establish biological relevance and clinical utility of our findings. Incorporating cytogenetics could help to identify aggressive subclones.[35]

Despite these limitations, this study provides one of the first comprehensive descriptions of CTPC phenotypes across disease stages and could establish a framework for further investigation. CTPC phenotyping supported by orthogonal data, such as recent single-cell transcriptomic profiling of CTPC,[36] will be essential to determine whether phenotypic features add predictive value beyond CTPC counts in discriminating progression patterns. Given its minimally invasive nature compared with BM sampling and the widespread availability of flow cytometry, this approach has the potential to deepen our understanding of progression patterns and also investigate therapeutic target availability in NDMM and treated MM.

Disclosures

BB reports ad hoc reviewing activities for Janssen-Cilag and has received honoraria from Janssen-Cilag, GSK, Amgen, Sanofi, Takeda, Pfizer, and Oncopeptides. All other authors have no conflicts of interest to disclose.

Contributions

SAB and AMPS designed the study. AMPS designed the experiments. SAB, AMPS, MP, and LMK analyzed and interpreted the data. LMK, SG, and CW performed experiments. SAB and MP prepared the manuscript. BB supported in data analysis and correlation with clinical data. All contributing authors collected and curated data, revised and approved the manuscript. All authors have read and agreed to the published version of the manuscript.

Acknowledgments

We thank all participants for donating blood. We would also like to thank Prof. Dr. Claudia Lengerke and all the hospital staff who supported our study. Moreover, we thank all members of the Flow Cytometry Core Facility at the University Hospital Tübingen.

Funding

This project received funding by the Nachwuchsgruppenprogramm of the Medical Faculty Tübingen (to AMPS). We acknowledge support by Open Access Publishing Fund of University of Tübingen.

Data-sharing statement

Data are available on request from the corresponding author.

References

1. Weiss BM, Abadie J, Verma P, et al. A monoclonal gammopathy precedes multiple myeloma in most patients. Blood. 2009;113(22):5418-5422.
2. Landgren O, Kyle RA, Pfeiffer RM, et al. Monoclonal gammopathy of undetermined significance (MGUS) consistently precedes multiple myeloma: a prospective study. Blood. 2009;113(22):5412-5417.
3. Dhodapkar MV. The immune system in multiple myeloma and precursor states: Lessons and implications for immunotherapy and interception. Am J Hematol. 2023;98 Suppl 2(Suppl 2):S4-S12.

4. Dang M, Han G, Lee HC, et al. Single cell clonotypic and transcriptional evolution of multiple myeloma precursor disease. Cancer Cell. 2023;41(6):1032-1047.e4.
5. Maeng CV, Rögnvaldsson S, Einarsson Long T, et al. Revised free light chain reference intervals enhance risk stratification in monoclonal gammopathy of undetermined significance and reduce overdiagnosis. Blood Cancer J. 2025;15(1):80.
6. Mateos M-V, Kumar S, Dimopoulos MA, et al. International Myeloma Working Group risk stratification model for smoldering multiple myeloma (SMM). Blood Cancer J. 2020;10(10):102.
7. Sanoja-Flores L, Flores-Montero J, Pérez-Andrés M, et al. Detection of circulating tumor plasma cells in monoclonal gammopathies: methods, pathogenic role, and clinical implications. Cancers (Basel). 2020;12(6):1499.
8. Gonsalves WI, Jevremovic D, Nandakumar B, et al. Enhancing the R-ISS classification of newly diagnosed multiple myeloma by quantifying circulating clonal plasma cells. Am J Hematol. 2020;95(3):310-315.
9. Bertamini L, Grasso M, D'Agostino M, et al. Poor prognosis of multiple myeloma predicted by high levels of circulating plasma cells is independent from other high-risk features but is modulated by the achievement of minimal residual disease negativity. Blood. 2020;136(Suppl 1):12-13.
10. Kostopoulos IV, Ntanasis-Stathopoulos I, Rousakis P, et al. Circulating plasma cells in newly diagnosed multiple myeloma: prognostic and more. J Clin Oncol. 2023;41(3):708-710.
11. Papadimitriou K, Tsakirakis N, Malandrakis P, et al. Deep phenotyping reveals distinct immune signatures correlating with prognostication, treatment responses, and MRD status in multiple myeloma. Cancers (Basel). 2020;12(11):3245.
12. Stern S, Chaudhuri S, Drayson M, et al. Investigation and management of the monoclonal gammopathy of undetermined significance. Br J Haematol. 2023;202(4):734-744.
13. Avet-Loiseau H, Davies FE, Samur MK, et al. International Myeloma Society/International Myeloma Working Group consensus recommendations on the definition of high-risk multiple myeloma. J Clin Oncol. 2025;43(24):2739-2751.
14. Park LM, Lannigan J, Jaimes MC. OMIP-069: Forty-color full spectrum flow cytometry panel for deep immunophenotyping of major cell subsets in human peripheral blood. Cytometry A. 2020;97(10):1044-1051.
15. Flores-Montero J, Sanoja-Flores L, Paiva B, et al. Next generation flow for highly sensitive and standardized detection of minimal residual disease in multiple myeloma. Leukemia. 2017;31(10):2094-2103.
16. Kostopoulos IV, Ntanasis-Stathopoulos I, Rousakis P, et al. Low circulating tumor cell levels correlate with favorable outcomes and distinct biological features in multiple myeloma. Am J Hematol. 2024;99(10):1887-1896.
17. Schinke C, Poos AM, Bauer M, et al. Characterizing the role of the immune microenvironment in multiple myeloma progression at a single-cell level. Blood Adv. 2022;6(22):5873-5883.
18. Všianská P, Říhová L, Varmužová T, et al. Analysis of B-cell subpopulations in monoclonal gammopathies. Clin Lymphoma Myeloma Leuk. 2015;15(4):e61-71.
19. Matsui W, Wang Q, Barber JP, et al. Clonogenic multiple myeloma progenitors, stem cell properties, and drug resistance. Cancer Res. 2008;68(1):190-197.
20. Tiedemann RE, Tagoug I, Erdmann N, et al. Multiple myeloma B cells and pre-plasma cells are important reservoirs for myeloma relapse following plasma cell-directed therapy and prevent cure with standard therapies. Blood. 2023;142(Suppl 1):642.
21. Bertamini L, Oliva S, Rota-Scalabrini D, et al. High levels of circulating tumor plasma cells as a key hallmark of aggressive disease in transplant-eligible patients with newly diagnosed multiple myeloma. J Clin Oncol. 2022;40(27):3120-3131.
22. Kastritis E, Kostopoulos IV, Theodorakakou F, et al. Prognostic significance of circulating plasma cells detected by next generation flow cytometry in light (AL) chain amyloidosis. Blood. 2022;140(Suppl 1):1150-1151.
23. Bal S, Kumar SK, Fonseca R, et al. Multiple myeloma with t(11;14): unique biology and evolving landscape. Am J Cancer Res. 2022;12(7):2950-2965.
24. Lee HJ, Song IH, Park IA, Heo S-H, Kim Y-A, Ahn J-H, Gong G. Differential expression of major histocompatibility complex class I in subtypes of breast cancer is associated with estrogen receptor and interferon signaling. Oncotarget. 2016;7(21):30119-30132.
25. Burugu S, Gao D, Leung S, Chia SK, Nielsen TO. TIM-3 expression in breast cancer. Oncoimmunology. 2018;7(11):e1502128.
26. Rani A, Murphy JJ. STAT5 in cancer and immunity. J Interferon Cytokine Res. 2016;36(4):226-237.
27. Wingelhofer B, Neubauer HA, Valent P, et al. Implications of STAT3 and STAT5 signaling on gene regulation and chromatin remodeling in hematopoietic cancer. Leukemia. 2018;32(8):1713-1726.
28. Ray A, Das DS, Song Y, et al. A novel agent SL-401 induces anti-myeloma activity by targeting plasmacytoid dendritic cells, osteoclastogenesis and cancer stem-like cells. Leukemia. 2017;31(12):2652-2660.
29. Ehrlich LA, Chung HY, Ghobrial I, et al. IL-3 is a potential inhibitor of osteoblast differentiation in multiple myeloma. Blood. 2005;106(4):1407-1414.
30. Giuliani N, Lisignoli G, Colla S, et al. CC-chemokine ligand 20/macrophage inflammatory protein-3α and CC-chemokine receptor 6 are overexpressed in myeloma microenvironment related to osteolytic bone lesions. Cancer Res. 2008;68(16):6840-6850.
31. Wang YN, Gan SL, Wu FF, et al. [Expression of CC-chemokine receptor 7 in patiens with multiple myeloma and its relationship with extramedullary disease]. Zhongguo Shi Yan Xue Ye Xue Za Zhi. 2017;25(2):476-479.
32. Schneider Revueltas E, Ferreira-Gomes M, Guerra GM, et al. Surface CD69-negative CD4 and CD8 bone marrow-resident human memory T cells. Eur J Immunol. 2025;55(5):e202451529.
33. Diamond BT, Baughn LB, Poorebrahim M, et al. Biallelic antigen escape is a mechanism of resistance to anti-CD38 antibodies in multiple myeloma. Blood. 2025;146(13):1575-1585.
34. Paiva B, Puig N, Cedena MT, et al. Differentiation stage of myeloma plasma cells: biological and clinical significance. Leukemia. 2017;31(2):382-392.
35. Lightbody ED, Sklavenitis-Pistofidis R, Wu T, et al. SWIFT-seq enables comprehensive single-cell transcriptomic profiling of circulating tumor cells in multiple myeloma and its precursors. Nat Cancer. 2025;6(9):1595-1611.
36. Garcés J-J, Simicek M, Vicari M, et al. Transcriptional profiling of circulating tumor cells in multiple myeloma: a new model to understand disease dissemination. Leukemia. 2020;34(2):589-603.